

Optimization and Characterization of Extruded Partially Pregelatinized Cassava Starch as Filler-Binder.

Gabriela Kasih Mawarni^{1,2}, Rumiya³, Teuku Nanda Saifullah Sulaiman^{4*}

1. Master in Pharmaceutical Sciences, Faculty of Pharmacy, Universitas Gadjah Mada, Jl. Sekip Utara, Sleman, Yogyakarta 55281, Indonesia.
2. National Research and Innovation Agency, B.J. Habibie Building, Jl. M.H. Thamrin No. 8, Central Jakarta 10340, Indonesia
3. Department of Pharmaceutical Chemistry, Faculty of Pharmacy, Universitas Gadjah Mada, Sekip Utara, Sekip Utara 55281 Yogyakarta, Indonesia.
4. Department of Pharmaceutical Technology, Faculty of Pharmacy, Universitas Gadjah Mada, Sekip Utara, Sekip Utara 55281 Yogyakarta, Indonesia.

Article Info

Submitted: 18-07-2022

Revised: 28-11-2022

Accepted: 22-12-2022

*Corresponding author
Teuku Nanda Saifullah
Sulaiman

Email:
tn_saifullah@ugm.ac.id

ABSTRACT

When using starch as a filler-binder, pregelatinization method by extrusion can enhance the flow characteristics and compressibility of the starch. This study aimed to find the optimum process parameter for producing partially pregelatinized cassava starch (PPCS) using twin screw extrusion and characterizing it as a filler-binder excipient. For the experimental trials, a three-level Box-Behnken design was used to make PPCS. The Box-Behnken design has three independent variables: starch moisture content (20%- 40%), extrusion temperature (50°C-70°C), and screw speed (10 rpm-30 rpm). The response surface methodology approach was used for optimization. The desired filler-binder characteristic of PPCS was defined as having good flowability and compactibility properties. The most desirable process parameter was achieved by combining 39.9 percent starch moisture content, 70°C extrusion temperature, and 25.8 rpm screw speed. The results showed that optimized PPCS has good flow properties and also good water absorption capacity. The optimized PPCS had a polygonal shape and a size range of 149-400µm. PPCS showed birefringence characteristics under polarized light, indicating a large number of undamaged starch granules. The PPCS XRD pattern showed peaks at 15°, 17°, 18°, and 23°, and also a relative crystallinity of 27.3 percent. When analyzed with DSC, PPCS revealed glass transition curves and a gelatinization degree of 11.8 percent.

Keywords: cassava starch, twin screw extrusion, partially pregelatinized, filler-binder, response surface methodology.

INTRODUCTION

The simplest method for creating tablets is by direct compression method. This method only requires the steps of weighing, mixing, and tableting, which decrease the use of machinery, energy, processing time, and labour, resulting in lower cost of tablets production (Iqubal et al., 2014). Because of their poor flowability and compressibility, not all active ingredients can be turned into tablets using the direct compression method, so additional material is required as a filler and a binder so that the powder mass can be compacted after compression. The development of a cost-effective and reliable filler-binder excipient

would be advantageous for pharmaceutical industry in terms of production. One promising breakthrough for filler-binder excipients is a modified form of starch such as cassava starch, which is a relatively low-cost resource in Indonesia.

Starch, a biopolymer in the form of granules, has been used by the pharmaceutical industry for a long time as a filler, binder, and disintegrant in solid dose formulations. However, because of its poor flowability and compressibility, which causes lamination and capping when compressed, its usage in formulations is limited (Jivraj et al., 2000; Rojas et al., 2012). Naturally, these challenges

must be solved in order to transform starch into filler-binder excipients by transforming the starch granules physically, chemically, and/or enzymatically. Pregelatinization is a technique for physically modifying starch granules that involves heating in the presence of water and then spray-drying, roll-drying, or drum-drying, extruding, or drying by using dry heat to destroy some or all of the starch granules (Park & Kim, 2021). By increasing the starch densification, this modification can improve the starch's compressibility. Furthermore, the pregelatinized starch particle size is greater than native starch, which improves the starch's flow characteristics (Rashid et al., 2013).

Starch 1500® is a commercialized partially pregelatinized corn starch (Short & Verbanac, 1978). However, cassava starch is used in this study because it is one of the most abundant sources of starch in Indonesia, with granules size similar to corn starch but less amylose content (Swinkels, 1985). In earlier investigations (Putra (2011) and Karisma Sari et al. (2012)), pregelatinized cassava starch was produced using a conventional heating process and showed to have good filler-binder properties. This study, however, intends to optimize the production of PPCS using the extrusion method. Extruder can be utilized in batch mode and is also well-suited to continuous processing. Using an extruder as a continuous processor is especially helpful when aiming to reduce manufacturing plant size and costs (Agarwal & Chauhan, 2019). Additionally, the extrusion method enables control of the degree of gelatinization through temperature and heating time control (Cheng et al., 2022).

In order to obtain a suitable PPCS for filler-binder excipients, the extrusion conditions need to be optimized for the process parameters that affect the final product. The optimization in this study used a statistical approach with Design of Experiment (DoE) to see the effect of extrusion process parameters, such as starch moisture content, extrusion temperature, and extruder screw speed, on the characteristics of PPCS. Using a Response Surface Methodology (RSM) that allows optimization of several independent variables at once, the experimental design was based on the Box-Behnken Design (BBD) with 3 levels and resulted in 15 runs including 3 repetitions at the centre point (Bezerra et al., 2008). This study also included the verification of the optimization and characterization of PPCS results.

MATERIALS AND METHODS

Cassava starch used for this study was from Lampung, obtained from PT. Tedco Agri. The chemicals used were Starch 1500® as benchmark and distilled water. This study used several instruments: a twin screw extruder Rheomex PTW24 (Thermo Scientific, Germany), a twin screw volumetric powder feeder (DDRS20, Brabender, Germany), an oven, a grinder, a PTG S4 flowability tester (PharmaTest, Germany), a HR-2000 powder integrative characteristic tester (Hengrui, China), a magnetic stirrer, a centrifuge, a water bath, a single-punch tablet press, a water absorption equipment, a scanning electron microscopy (Hitachi, Japan), a polarized light microscope (Zeiss Primotech, Germany), an AERIS-Benchtop diffractometer (PAN Analytical, Netherland), and a DSC 3+ (Mettler Toledo, Germany).

PPCS Preparation

Cassava starch was pre-mixed with water to attain the desired moisture content before being extruded. PPTS was produced using an intermeshing co-rotating twin screw extruder Rheomex PTW24 (Thermo Scientific, Germany) with a 24 mm diameter barrel, length to diameter ratio of 28:1, seven temperature zones, and cylindrical dies (2.8 mm). Screw configuration consists entirely of conveying components. Cassava starch was fed into the extruder with a twin screw volumetric powder feeder (DDRS20, Brabender, Germany) at total feed rate 10 g/min through the hole in the center of the extruder barrel so that the L/D ratio of the extruder was reduced by half and the heating zones used were four (including the die zone; the temperature was set to 10 degrees lower). Extrusion temperature and screw speed were set according to DoE (Table I).

After 30 min from the initial output of the extruder, the extrudate was collected and cut manually. The extruded product was then dried in an oven at 40°C until the extrudate was dry enough to grind. The extrudate particles were then sieved to obtain powder particles that passed through a 40 mesh sieve but were retained on a 100 mesh sieve. Finally, the amount of moisture in the PPCS powder was reduced to under 5%.

Experimental Design

Three levels each of starch moisture content (A: 30%, 35% and 40%), extrusion temperature (B: 50°C, 60°C, and 70°C), and screw speed (C: 10 rpm, 20 rpm, and 30 rpm) were chosen as the independent variables based on preliminary

Table I. Box-Behnken Design for three factors with the results

Std	Independent variables			Dependent variables (Y)								
	A	B	C	Y ₁	Y ₂	Y ₃	Y ₄	Y ₅	Y ₆	Y ₇	Y ₈	Y ₉
1	30	50	20	3.8±0.0	32.7±0.1	0.65±0.01	0.78±0.01	16.5±2.5	1.20±0.04	5.0±0.1	2.7±0.6	0.6245±0.0106
2	40	50	20	3.8±0.1	30.8±0.2	0.64±0.01	0.75±0.00	14.7±2.5	1.17±0.03	5.5±1.0	8.2±2.0	0.5367±0.0055
3	30	70	20	3.9±0.0	31.4±0.3	0.61±0.00	0.73±0.01	16.7±1.5	1.20±0.02	4.5±0.2	0.5±0.2	0.6564±0.0061
4	40	70	20	3.9±0.0	31.2±0.3	0.60±0.01	0.72±0.01	17.0±1.0	1.20±0.01	5.7±0.1	0.6±0.0	0.6101±0.0032
5	30	60	10	3.8±0.0	32.1±0.2	0.63±0.00	0.76±0.01	17.0±1.0	1.20±0.01	8.2±0.2	7.0±1.3	0.7209±0.0078
6	40	60	10	3.8±0.1	32.6±0.4	0.63±0.00	0.77±0.01	17.7±0.6	1.21±0.01	6.9±0.3	7.9±2.3	0.6216±0.0160
7	30	60	30	5.3±0.1	31.6±0.7	0.44±0.01	0.55±0.01	19.7±0.6	1.24±0.01	0.0±0.0	0.0±0.0	0.2971±0.0060
8	40	60	30	4.3±0.1	32.2±0.1	0.54±0.00	0.66±0.01	17.8±0.8	1.22±0.01	1.8±0.0	0.2±0.0	0.5125±0.0117
9	35	50	10	4.0±0.0	32.0±0.2	0.60±0.01	0.72±0.00	16.7±1.5	1.20±0.02	4.2±0.4	0.6±0.1	0.5628±0.0192
10	35	70	10	4.0±0.0	32.2±0.2	0.60±0.00	0.74±0.01	19.0±1.0	1.23±0.02	4.4±0.2	0.7±0.2	0.5796±0.0175
11	35	50	30	5.8±0.1	33.3±0.6	0.41±0.01	0.51±0.00	20.3±0.6	1.26±0.01	0.1±0.1	0.0±0.0	0.2734±0.0217
12	35	70	30	3.7±0.1	31.5±0.2	0.64±0.00	0.76±0.01	16.7±1.5	1.20±0.02	6.1±0.2	6.5±1.3	0.5691±0.0004
13	35	60	20	5.2±0.1	31.6±0.1	0.46±0.00	0.56±0.01	17.8±1.3	1.22±0.02	0.4±0.3	0.0±0.0	0.2974±0.0090
14	35	60	20	4.0±0.1	32.5±0.1	0.60±0.00	0.72±0.00	16.2±0.8	1.19±0.01	4.9±0.1	0.5±0.2	0.6125±0.0083
15	35	60	20	4.7±0.1	31.1±0.3	0.52±0.00	0.63±0.00	17.3±0.6	1.21±0.01	2.5±0.2	0.2±0.1	0.4812±0.0089

A : starch moisture content (%); B : extrusion temperature (°C); C : screw speed (rpm); Y₁ : flow time (second/100 g); Y₂ : angle of repose (°); Y₃ : bulk density (g/ml); Y₄ : tapped density (g/ml); Y₅ : Carr Index (%); Y₆ : Hausner Ratio; Y₇ : cold water solubility (%); Y₈ : compressibility (kg); Y₉ : water absorption (g/250 mg).

investigations and the literature utilizing the DoE with response surface and Box-Behnken Design (Table I). Flow time (Y₁), angle of repose (Y₂), bulk density (Y₃), tapped density (Y₄), Carr Index (Y₅), Hausner Ratio (Y₆), cold water solubility (Y₇), compactibility (Y₈), and water absorption (Y₉) were chosen as dependent variables/ responses.

Version 13 of Design Expert® software (Stat-Ease Inc., Minneapolis, MN, USA) was used to evaluate the data. Multiple linear regression analysis (MLRA) was used to create models for each dependent variable, and each model was then assessed using a set of statistical parameters. With a 95% level of confidence (p = 0.05), the F test or p value of the analysis of variance (ANOVA) was used to establish whether the independent variables had a significant impact on dependent variables. In order to explain the interaction effects of independent variables on dependent variables, a perturbation plot based on the equation of dependent variables was created. Optimization was accomplished through numerical optimization, which was calculated within the software.

Characterization of cassava starch and PPCS

Flow time and angle of repose were determined using 100 g of powder poured into a funnel on the PTG S4 Flowability Tester (PharmaTest, Germany) with a certain diameter

(15 mm for flow time and 6 mm for angle repose) opening at the bottom of the funnel. After pressing the start analysis button, the funnel's bottom cover automatically opened to begin measuring the flow rate and angle of repose (Okunlola, 2018).

Bulk (D_a) and tapped densities (D_c) were determined using 100 mL (V₀) of powder poured carefully into clean and dry graduated cylinder. Then, the graduated cylinder containing the powder was tapped using the HR-2000 Powder Integrative Characteristic Tester (Hengrui, China) for 1250 taps and the volume (V₁₂₅₀) was recorded and powder was weighed. The bulk and tapped densities were calculated by dividing the powder's weight and volume (V₀ and V₁₂₅₀, respectively) (U.S. Pharmacopeia, 2018). The formulas established in Eq. (1) and (2) were used to determine Carr Index and Hausner Ratio respectively (Suñé Negre et al., 2013).

$$Carr\ Index\ (\%) = \frac{(D_c - D_a)}{D_c} \times 100 \dots \dots \dots (1)$$

$$Hausner\ Ratio = \frac{D_c}{D_a} \dots \dots \dots (2)$$

Cold-water-soluble matter was determined using 3,000 g of powder (m_s), and it was then slowly added to a beaker with 100 mL of water at 25°C and stirred for 5 min with a magnetic stirrer. Then, the dispersion was centrifuged at 3500 rpm for 30 min. The 25 mL supernatant (clear

component) was pipetted into a crucible that had been weighed precisely to 0.1 mg after being dried in an oven at $120 \pm 2^\circ\text{C}$ for four h (m_1). After the supernatant had been mostly evaporated over a water bath, the crucible was heated in an oven at 120°C for four h before being cooled in a desiccator. The crucible was weighed once more after cooling and steady weighting (m_2). The percentage of cold-water-soluble matter was calculated using Eq. 3 (Council of Europe, 2010). Moisture content data of sample powder (mc) was needed in this equation.

$$CWS (\%) = \frac{(m_2 - m_1) \times 100 / 25}{m_s \times (100 - mc) / 100} \times 100 \dots\dots\dots(3)$$

Utilizing a single-punch tablet press, the powder was compressed using upper and lower punches of 7 mm and 10 mm scale pressure. The hardness of the produced tablet was used to evaluate the powder' compactibility (Sulaiman et al., 2022).

Water absorption analysis was performed using water absorption equipment coupled with an ampoule on top of an electrical balance. Water was added to the ampoule until its surface was at the same level as that of the water on the tube of the water absorption equipment. On the tube apparatus, samples of powder were put in the holder covered by filter paper. After 15 min, the water loss on ampoules from 250 mg samples was calculated (Sulaiman et al., 2022).

The surface morphology of cassava starch and optimized PPCS were observed using scanning electron microscopy/SEM (Hitachi, Japan) at an accelerating voltage of 5 keV (Odeku & Picker-Freyer, 2009). Besides that, the starch granule morphologies were observed under polarized light microscope (Zeiss Primotech, Germany).

The structure of cassava starch and optimized PPCS were characterized by X-rays diffraction (XRD) using an AERIS-Benchttop diffractometer (PAN Analytical, Netherland), with monochromatic $\text{CuK}\alpha$ radiation of wavelength 1.54 Å, at 25°C . To ensure that the PPCS gave an intense pattern, PPCS had to be powdered and sieved through a 200 mesh sieve before examination (Lund & Lorenz, 1984). At a voltage of 40 kV and a current of 15 mA, the analysis was carried out over a range of 2θ between 5° and 85° and step size 0.022. The relative crystallinity of starch was determined by dividing the peak area belonging to the crystalline phase by total area under the XRD curve that was calculated using Origin software (v.7.5, Microcal Inc., USA) (Dome et al., 2020).

A DSC 3+ (Mettler Toledo, Germany) was used to evaluate the thermal behavior of starch gelatinization. Preliminary, the device was calibrated using metal indium (99.999 percent). In an aluminum pan, the sample and water were precisely weighed in a 1:3 ratio. Sample and water were mixed homogeneously before the pan was sealed. The sample pans were equilibrated at room temperature for 4 h then was placed into DSC chamber with an empty pan as the reference. Temperature was maintained at 30°C for one minute, then escalated to 90°C with a $16^\circ\text{C}/\text{min}$ scanning rate. During the analysis, nitrogen gas stream was enabled to fill the DSC chamber at a rate of 30 mL/min (Wootton & Bamunuarachchi, 1978; X. Zhang et al., 2013). The onset temperature (T_o), peak temperature (T_p), conclusion temperature (T_c) and gelatinization enthalpy (ΔH_g) were determined by a Star^e software (Mettler Toledo).

RESULTS AND DISCUSSION

Fifteen experiments were carried out in accordance with the DoE (Table I). The results (Table I) were analyzed using RSM and Design Expert 13 software to determine the regression model's fitting parameters. The goodness of fit statistics of the models for dependent variables are given in supplementary data. The perturbation plot model is a schematic representation of the comparison of all factors' impacts at a specific DoE point. Compared to contour plots and 3D graphs, this axis arrangement offers greater flexibility (Mishra et al., 2008).

Influence of independent variables on flow time

Flow time of 100 g of PPCSs were less than 10 s and less than 20 s for the 10-mm outlet nozzle (data not shown) in all experiments, indicating good flow characteristics. The flow characteristics of PPCS powders were greatly influenced by particle size greater than $150 \mu\text{m}$ (retaining 100 mesh) (Kaleem et al., 2021). Based on the design of experiment approach, the impact of the independent variable on the flow time response is described by a quadratic model shown in Eq. 4.

$$\text{Flow time} = 27.86 - 0.59A - 0.52B + 0.42C + 3.171 \times 10^{-3}AB - 6.919 \times 10^{-3}AC - 3.893 \times 10^{-3}BC + 6.988 \times 10^{-3}A^2 + 3.533 \times 10^{-3}B^2 + 2.025 \times 10^{-3}C^2 \dots\dots\dots(4)$$

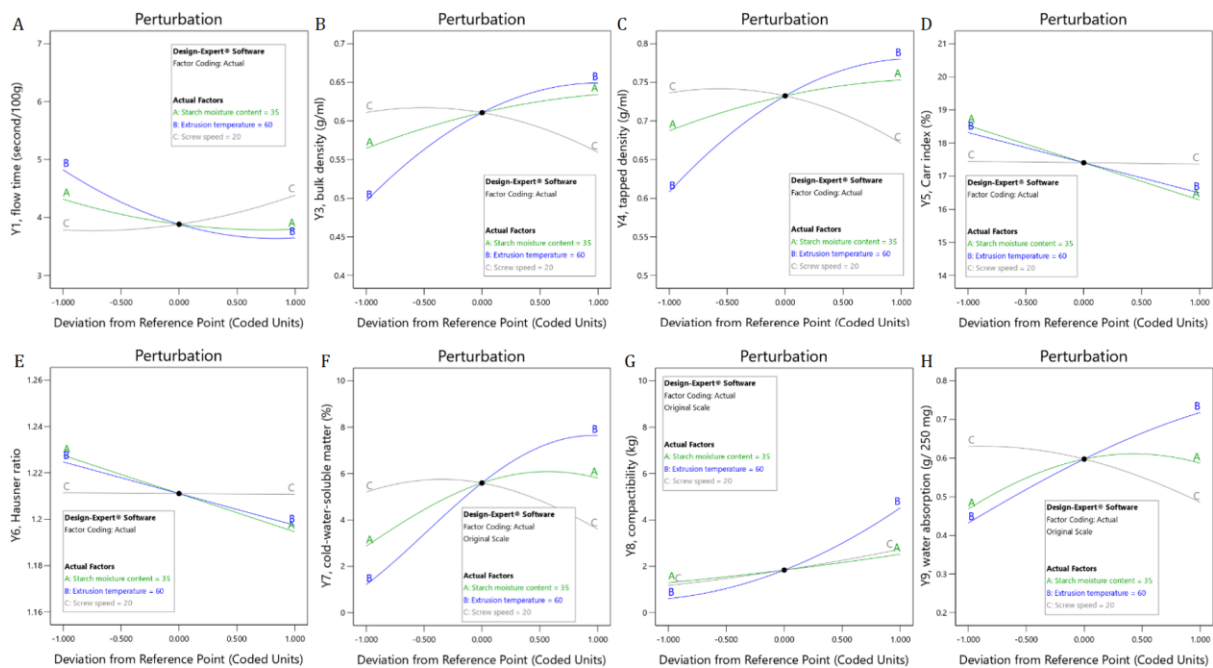


Figure 1. Perturbation plots showing the effect of each of the independent variables on dependent variables : (A) flow time, (B) bulk density, (C) tapped density, (D) Carr index, (E) Hausner ratio, (F) cold-water-soluble matter, (G) compactibility, and (H) water absorption.

According to Eq. 4, all independent variables have strong impact on flow time. Additionally, only the extruder screw speed (C) has a positive effect on the flow time because the coefficient is positive. In other words, a faster screw speed will result in a longer powder flow time. The perturbation plot demonstrates something similar (Figure 1(a)). Flow time is an inverse function of flow properties, i.e. the shorter the flow time, the better the powder's flow properties. Equation 4 can also be used to understand that a higher starch moisture content, a higher extrusion temperature, and a lower screw speed will all lead to a shorter flow time, which will lead to a greater increase in flow properties. This is similar to the findings of Karisma Sari et al. (2012), who found that increasing the temperature and the amount of water can increase the amount of gelatinized starch and hence the flowability of the powder.

Powder flow properties are influenced by particle density in addition to particle size. In comparison with denser particles, in general, less dense particles of the same size and shape tend to have lower cohesion, allowing them to flow freely with the help of gravity (Divya & Ganesh, 2019). Pregelatinization causes starches to become more dense (Rashid et al., 2013). The more gelatinized

the starch, the denser the starch particles are, and the better the flow properties are.

Influence of independent variables on angle of repose

The response of the angle of repose obtained from the DoE produces values in the range of $30.8 \pm 0.2^\circ$ – $33.3 \pm 0.6^\circ$. The results of the model suitability analysis were carried out on all data transformation; however, the results showed that none of the models could be utilized to predict optimum conditions. This implies that all independent variables have no effect on the angle of repose.

According to Beakawi Al-Hashemi & Baghabra Al-Amoudi (2018), the particle's size and shape have an impact on the angle of repose. In this study, the PPCS was sieved to create particles with a size range of 149 μm to 400 μm . Because particle size had no impact on the independent variable, the DoE approach was not applicable.

Influence of independent variables on bulk density and tapped density

All PPCS had bulk density ranging from 0.41 ± 0.01 to 0.65 ± 0.01 g/mL and tapped density ranging from 0.51 ± 0.00 to 0.78 ± 0.01 g/mL.

According to ANOVA test (supplementary data), the quadratic model was significant and adequately explained bulk density and tapped density data. The equations obtained based on the analysis of models and variances are shown in Eq. 5 and Eq. 6.

$$\begin{aligned} \text{Bulk density} = & -1.631 + 4.029 \times 10^{-2}A + 5.597 \times 10^{-2}B - 4.677 \times \\ & 10^{-2}C - 3.12 \times 10^{-4}AB + 8.57 \times 10^{-4}AC + 4.07 \times 10^{-4}BC - \\ & 4.53 \times 10^{-4}A^2 - 3.79 \times 10^{-4}B^2 - 2.56 \times 10^{-4}C^2 \dots\dots\dots(5) \end{aligned}$$

$$\begin{aligned} \text{Tapped density} = & -1.53 + 4.229 \times 10^{-2}A + 5.764 \times 10^{-2}B - 5.464 \times 10^{-2}C - \\ & 3.55 \times 10^{-4}AB + 10.03 \times 10^{-4}AC + 4.63 \times 10^{-4}BC - 4.93 \\ & \times 10^{-4}A^2 - 3.82 \times 10^{-4}B^2 - 2.88 \times 10^{-4}C^2 \dots\dots\dots(6) \end{aligned}$$

Equations 5 and 6 have the same pattern. The extrusion temperature (coefficient B) has a more dominant effect on the bulk density than the others. Since the extrusion temperature (B) and the starch moisture content (A) have a positive coefficient, the increase causes the bulk density and tapped density to rise. Although an increase in the screw speed causes a decrease in response, the fact that the coefficients of linear effect (A, B, and C) are close to one another suggests that all independent variables have a significant impact on tapped density. Furthermore, the perturbation graph demonstrates this (Figures 1(b) and 1(c)). As previously mentioned, the pregelatinization process affects the density of starch particles, which is why the corresponding responses follow the same model pattern.

Influence of independent variables on Carr index and Hausner ratio

Bulk density and tapped density measurements were used to determine the Carr index and Hausner ratio (Eq. 1 and 2). The Carr index of PPCSs were between 14.7±2.5 and 20.3±0.6 percent. The Hausner ratio was between 1.17±0.03 and 1.26±0.01. Both results indicate that PPCSs had good flowability properties, according to U.S. Pharmacopeia (2018). The lower the Carr index and Hausner ratio, the better the powder's flow abilities.

The linear model for Carr index and Hausner ratio was expressed in equations 7 and 8. All independent variables have a negative impact according to model Eq. 7 & 8, with the starch moisture content (A) being the biggest factor of shifts in the Carr index value. In figures 1(d) and 1(e), the perturbation plot demonstrates that the

extruder screw speed (C) has little impact on the Carr index and Hausner ratio value. This is different from the findings of Karisma Sari et al. (2012) where the increase in temperature also decreases the Carr index.

$$\begin{aligned} \text{Carr index} = & 30.83 - 22.487 \times 10^{-2}A - 9.120 \times \\ & 10^{-2}B - 0.410 \times 10^{-2}C \dots\dots\dots(7) \end{aligned}$$

$$\begin{aligned} \text{Hausner Ratio} = & 1.41 - 3.295 \times 10^{-3}A - 1.365 \times 10^{-3}B \\ & - 0.032 \times 10^{-3}C \dots\dots\dots(8) \end{aligned}$$

Influence of independent variables on cold-water-soluble matter

The experimental design's response of cold-water soluble matter yields a value in the range of 0 - 8.2±0.2%. The combined effect of the independent variables on cold-water-soluble matter showed fitting according to the quadratic model as depicted in Eq. 9.

$$\begin{aligned} \sqrt{\text{Cold-water-soluble matter}} = & -46.02 + 1.36A + 0.86B - 0.49C - 9.84 \times 10^{-3}AB + \\ & 8.96 \times 10^{-3}AC + 4.49 \times 10^{-3}BC - 12.57 \times 10^{-3}A^2 - \\ & 4.37 \times 10^{-3}B^2 - 2.76 \times 10^{-3}C^2 \dots\dots\dots(9) \end{aligned}$$

According to coefficient of the model equation above, compared to the interaction and quadratic effects of the independent variables, the linear effect has a much greater impact on the percentage of cold-water-soluble matter PPCS. According to Eq. 9, the increase in cold-water soluble matter was caused by an increase in starch moisture content, an increase in extrusion temperature, and a decrease in screw speed. The perturbation plot (Figure 1(f)) illustrates the same concept.

Cold-water-soluble matter is also known as an index of water solubility (WSI) (Anderson et al., 1970). Ali et al. (2020) investigated the relationship between extrusion temperature and WSI, and the results demonstrate that the WSI increases with increasing extrusion temperature. Starch is partially soluble in cool water after being gelatinized during the extrusion process. High extrusion temperatures increase the amount of gelatinized starch, which raises the starch's water solubility. More specifically, the water solubility equation created by Cheng et al. (2022) shows that the interplay of three parameters: shear stress (which is directly related to screw speed), thermal-mechanical input (including extrusion temperature), and moisture content, determines the water solubility of the extrudate.

Influence of independent variables on compactibility

As previously mentioned, the hardness of the tablet created from PPCS was used to evaluate the compactibility of PPCS. The tablet's hardness varied from 0 to 8.2±0.2 kg. The outcomes of the model suitability analysis show that the two-factor interaction/ 2FI model was regarded as suitable. The mathematical equation for this model is shown in Eq. 10. In the perturbation plot (Figure 1(g)), the extrusion temperature (B) has a dominant effect on the compactibility. Karisma Sari et al. (2012) also found that raising the temperature and amount of water increased pregelatinized starch compressibility, decreased tablet friability, and increased tablet disintegration time.

$$\sqrt{\text{Compactibility}} = -6.16 + 0.252A + 0.249B - 0.841C - 0.817 \times 10^{-2}AB + 1.455 \times 10^{-2}AC + 0.610 \times 10^{-2}BC \dots\dots\dots(10)$$

Influence of independent variables on water absorption

The response of water absorption gained from the experimental design produced a value in the range of 0.2734±0.0217 – 0.7209±0.0078 g/250 mg sample or 1.09±0.09 – 2.88±0.03 mg water/mg sample. The cumulative influence of the independent variables on the water absorption fit the quadratic model, as shown by Eq. 11.

$$\sqrt{\text{Water absorption}} = -3.329 + 1.660 \times 10^{-1}A + 0.483 \times 10^{-1}B - 0.633 \times 10^{-1}C - 7.339 \times 10^{-4}AB + 9.917 \times 10^{-4}AC + 5.798 \times 10^{-4}BC - 1.909 \times 10^{-3}A^2 - 0.206 \times 10^{-3}B^2 - 0.276 \times 10^{-3}C^2 \dots\dots\dots(11)$$

Starch moisture content is the main variable that affects water absorption, as shown by equation 11. The pattern of Eq. 11 resembles that of Eq. 9, indicating that each factor's impact on cold-water-soluble matter is analogous to its impact on water absorption. This outcome differs slightly from that of Leonel et al. (2009), who found that the moisture content of the starch had no noticeable impact on the water absorption. This occurs as a result of the low starch moisture content (12.5-19.5%) in Leonel's study.

Conclusion of RSM analysis

According to Lund & Lorenz (1984), the pregelatinization process is influenced by several different factors, including temperature, time, and amount of water. The extrusion temperature is used as the heating temperature in the process, and

the heating time is defined by the residence time, which is directly correlated with the screw speed (Sørensen, 2012). Increasing the amount of water and temperature will increase the degree of gelatinization. According to the results, increasing starch's moisture content and temperature will lead to a decrease in flow time (which means increased flowability), an increase in bulk and tapped density, a decrease in the Carr index and Hausner ratio (which also means increased flowability), and also an increase in compressibility, percentage cold-water soluble matter, and water absorption. Screw speed is the opposite of this. As the screw speed increases, the residence time decreases, lowering the level of gelatinization. The RSM analysis results in a mathematical model with good predictive power on several responses (shown in supplementary data).

Optimization of PPCS

The goal of the optimization is to create PPCS with desirable filler-binder properties: (1) good flowability (flow time less than 10 s (Zhang et al., 2006), Carr index less than 25, (2) Hausner ratio less than 1.34 (U.S. Pharmacopeia, 2018)), (3) bulk density within the range of 0.5-0.7 (Short & Verbanac, 1978), (4) tapped density within the range of 0-1 (Suñé Negre et al., 2013), (5) cold-water-soluble matter less than 20%, (6) compactibility/ hardness tablet within the range of 4-8 kg (Short & Verbanac, 1978), and (7) higher water absorption in experimental runs. This can be successfully accomplished by modifying design parameters with the aid of a suitable numerical optimization approach (Table II).

Design Expert software version 13 was used for the optimization, which produced 52 solutions. The extrusion condition with the highest desirability (0.597) had a starch moisture content of 39.9%, an extrusion temperature of 70°C, and a screw speed of 25.8 rpm, along with the predicted PPCS properties (Table II). The highest desirability was not excessively high since the optimal condition's desirability value on the dependent variable's Carr index and Hausner ratio was less than 0.5 (0.401 and 0.467 respectively). An extra batch experiment was performed using the recommended condition to validate the model's prediction and the reliability of the optimal combination. As a result, it can be concluded from Table II that the optimized PPCS is not as precise as the prediction.

Table II. Optimization requirements with predicted values and actual values of dependent variables

Response component	Goal	Lower Limit	Upper Limit	Importance	Prediction	Verification	Unit
Flow time	minimize	1	10	3	3.537	4.0±0.0	s/100g
Angle of repose	-	-	-	-	-	32.5±0.1	°
Bulk density	is in range	0.5	0.7	3	0.681	0.61±0.01	g/mL
Tapped density	is in range	0	1	3	0.81	0.75±0.01	g/mL
Carr index	minimize	1	25	3	15.378	19.0±1.0	%
Hausner ratio	minimize	1	1.34	3	1.181	1.23±0.02	-
Cold-water-soluble matter	is in range	0	20	3	7.011	5.6±0.0	%
Compactibility	is in range	4	8	3	8.52	1.1±0.2	kg
Water absorption	maximize	0.2734	0.7209	3	0.69	0.7729±0.0040	g/250 mg

Table III. Comparison of optimized PPCS with other pregelatinized starch

Response component	Unit	PPCS Verification	Starch 1500®	Putra (2011)	Sari et al. (2012)	Sulaiman et al. (2022)
Flow time	s/100g	4.0±0.0	Not fall	5.4±0.2	7.3	6.0
Angle of repose	°	32.5±0.1	28.8±0.4	26.1±0.6	25.6±0.3	32.7
Bulk density	g/mL	0.61±0.01	0.68±0.01	0.53±0.00	-	-
Tapped density	g/mL	0.75±0.01	0.92±0.00	0.63±0.00	-	-
Carr index	%	19.0±1.0	25.7±0.6	15.4±0.5	8.5±1.3	24
Hausner ratio	-	1.23±0.02	1.35±0.01	1.18±0.01	-	-
Cold-water-soluble matter	%	5.6±0.0	14.8±0.2	-	-	-
Compactibility	kg	1.1±0.2	2.7±0.2	5.0±1.0	8.8±0.2	3.42
Water absorption	g/250 mg	0.7729±0.0040	0.9889±0.0308	0.525±0.001	-	6.64
Particle size	µm	149-400	~65	52.85	250-850	50-100
Starch source		Cassava	Corn	Cassava	Cassava	Sago
Gelatinization process		Twin screw extrusion, 39.9% moisture content, 70°C, 25.8 rpm screw speed		Heating, starch : water 1:1, 80°C, 10 min	Heating, starch : water 1:1, 60°C, 10 min	Heating, starch : water 1:1, 85°C, 60 min

Characterization of the optimized PPCS

The optimized PPCS was evaluated in comparison to the predicted value (Table II), Starch 1500® as a benchmark that has been used by the pharmaceutical industry, and other pregelatinized starch (Table III). Overall, the verification value is quite similar to the predictive value. The optimized PPCS has good flowability according to value of flow time, angle of repose, Carr index, and Hausner ratio. Although the actual Carr index and Hausner ratio of the optimized PPCS were greater than the predictive value, it still indicated a good flowability. The optimized PPCS cannot be compacted to be a tablet as strong as it is predicted.

This could be due to a large difference between the adjusted R² and the predicted R² of the statistical model (shown in supplementary data).

The flow time of the optimized PPCS was considerably better than Starch 1500® and other pregelatinized starch (Table III). Starch 1500® (moisture content = 10.0%) became trapped and failed to flow when flow time was recorded using a 15mm-outlet nozzle. Starch 1500® can only be measured with a flow time of 9.3 s for 100 g powder (flow rate 10.75 g/s) when the water content has been reduced to less than 5%. This outcome was similar to the findings of Getachew et al. (2020) who reported 10.50 g/s in their study.

The optimized PPCS has 32.5° angle of repose that has considerably good flow according to European Pharmacopoeia (2010). Starch 1500® has surprisingly lower angle of repose that is 28.8° (excellent flowability) and 25.56° as reported from the findings of Getachew et al. (2020). Other pregelatinized cassava starch has lower angle of repose than the optimized PPCS.

Actual bulk density of the optimized PPCS is close to Starch 1500® (0.648 g/mL; 0.621 g/mL in Getachew et al.'s study (2020)), but the optimized PPCS's tapped density was lower than Starch 1500® (0.920 g/mL). This time, Getachew et al. (2020) reported a different tapped density of Starch 1500®: 0.726 g/mL, which resulted in a difference in Carr index and Hausner ratio results with the value recorded in this work. Carr index and Hausner ratio of the optimized PPCS were smaller than Starch 1500®, which means that the optimized PPCS has better flowability.

Starch 1500® has a higher percentage of cold-water solubility (14.817%) than the optimized PPCS, indicating that it contains more gelatinized starch. Unfortunately, there is no data on the percentage of cold-water soluble matter in other pregelatinized starches.

Under the same conditions, Starch 1500® produced a tablet with a hardness of 2.73 kg, and cassava starch produced a capping tablet. As a comparison, pregelatinized sago starch created by Sulaiman et al. (2022) with smaller particle size can be compacted as a 3.42 kg hardness tablet. Although fine particles can reduce powder flowability, a lack of fine particles may contribute to weak interparticle binding, which reduces tablet strength (Šantl et al., 2011).

Water absorption of the optimized PPCS exceeds the prediction (3.09 mg water/mg powder). Although this value is higher than the cassava starch (0.76 mg/mg powder) and pregelatinized cassava starch made by Putra (2011), Starch 1500® can absorb more water (4.00 mg) per 1 mg powder. Surprisingly, pregelatinized sago starch produced by Sulaiman et al. (2022) can absorb 26.56 mg water per 1 mg powder (almost 6x greater than the optimized PPCS).

Morphological observation using SEM and polarized microscope reveals microstructure of starch particle. Under scanning electron microscope, cassava starch (Figure 2(b)) seemed to have similar size to corn starch (Figure 2(d)) but more rounded. The particle of the optimized PPCS (Figure 2(a)) has a polygonal shape and is larger

than the particle of Starch 1500®, which appears to have an irregular shape (Figure 2(c)). When examined closely, formations of cassava starch granules can be seen on the surface of the PPCS particle. When the PPCS was examined under polarized light, this discovery became clearer (Figure 2(e)). Native starch has unique behavior when examined under polarized light called birefringence. Birefringence is a characteristic of native starch that causes polarized light to refract twice, resulting in a unique pattern known as a "Maltese cross" (Figures 2(f) and 2(h)). Birefringence is related to the crystalline structure of starch granules. When granule starch is disorganized or deformed as a result of modification, it exhibits poor birefringence or no birefringence pattern at all (Jiang et al., 2010). Figure 2(e) shows that the particles of PPCS are made up of starch granules that resemble colorful beads, indicating a high crystalline structure. This indicates that even though the starch granules in PPCS particles were exposed to the gelatinization process, they were still largely undamaged. In contrast to PPCS, the Starch 1500® particle (Figure 2(g)) contains ghost remnants (as indicated by the yellow arrow) created from the damaged outer granule layer during the gelatinization process (Atkin et al., 1998).

Starch is made up of two types of polysaccharides: amylose and amylopectin. Amylose is a straight chain polysaccharide that makes up the granules' amorphous part. Amylopectin is a polysaccharide that is branching and forms the crystalline part of granules. Based on the XRD pattern, starch is often categorized into three types: type A, which is commonly found in cereal starch; type B, which is found in high-amylose starch; and type C, which is found in starch originating from legumes and plant roots. The XRD pattern of type C is a combination of types A and B crystalline structure, the intensity of which is determined by the proportion of the two kinds in starch granules (Dome et al., 2020). Dome et al. (2020) reported that cassava or tapioca starch has C-type crystalline structure that has diffraction peak at 15.15°, 17.2°, 18.19°, and 22.78° with relative crystallinity about 42%. Xia et al. (2015) reported slightly different findings, stating that cassava starch belongs to type A and contains diffraction peaks at 15°, 17°, 18°, and 23° with relative crystallinity about 24.67%. There were no diffraction peaks identified at 2θ greater than 30°, which is in line with Dome et al.'s (2020) findings.

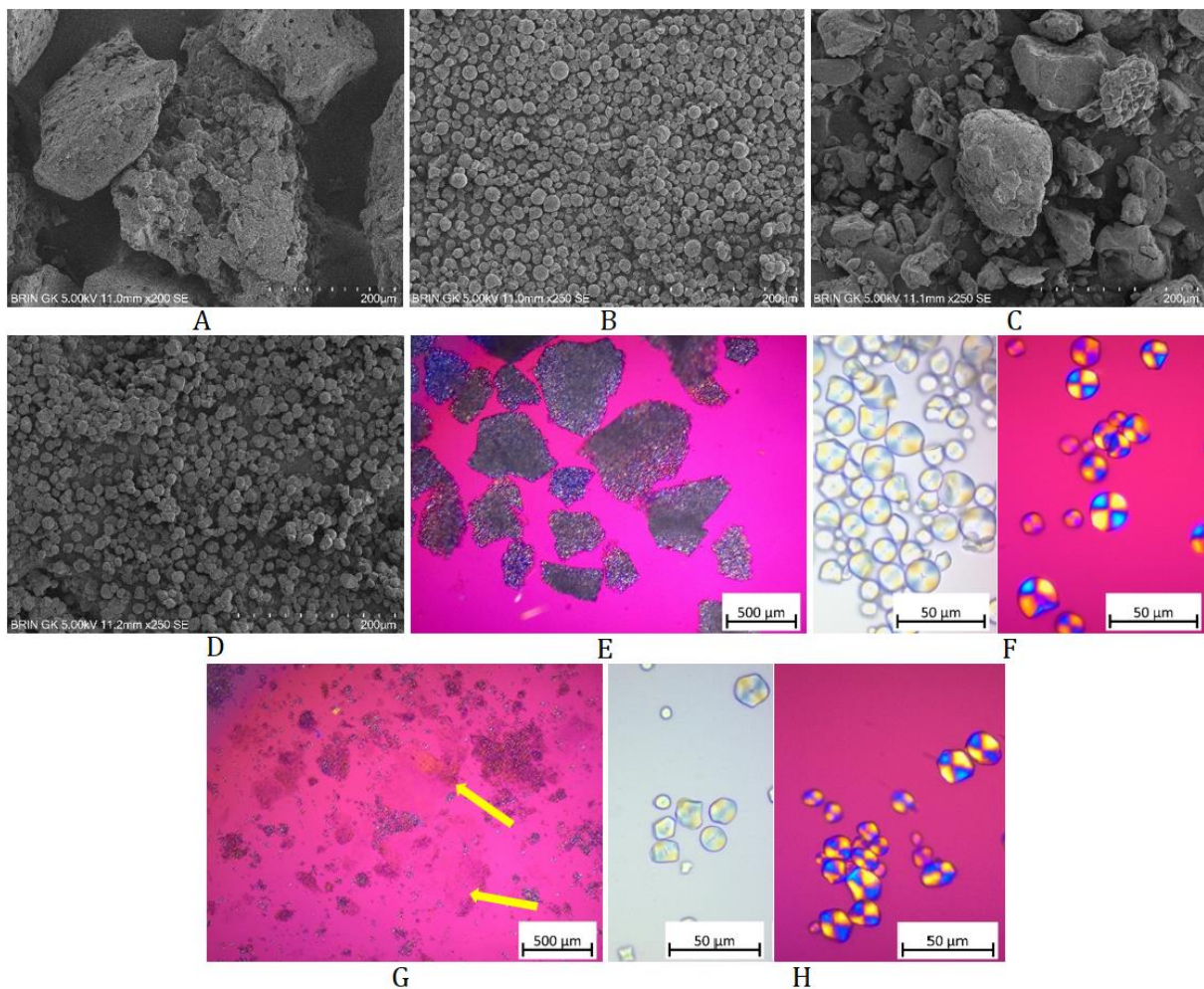


Figure 2. SEM images of (A) optimized PPCS (200x magnification), (B) cassava starch (250x magnification), (C) Starch 1500® (250x magnification), and (D) corn starch (250x magnification); polarized images of (E) optimized PPCS (50x magnification), (F) cassava starch (630x magnification), (G) Starch 1500® (50x magnification), and (H) corn starch (630x magnification)

According to the abovementioned data, the diffraction peaks of the cassava starch and the optimized PPCS appeared at 15°, 17°, 18°, and 23° (Figure 3(a)) with relative crystallinity about 50.8% and 27.3% respectively. These results show that the optimum conditions for PPCS cause cassava starch to lose 23.5% of its crystallinity. According to Rashid et al. (2013), keeping the crystallinity as high as possible is one of the keys to the success of creating physically modified starch into filler-binder excipients because an increase in the percentage of relative crystallinity has a positive impact on tablet strength. Starch 1500® and corn starch both

seemed to have peaks that were similar to those of cassava starch, though Starch 1500®'s peak intensity was much lower and its relative crystallinity to corn starch was about 23.6% lower than corn starch's relative crystallinity (39.4%).

DSC study revealed the thermal behavior of cassava starch, optimized PPCS, maize starch, and Starch 1500®. Endothermic curve suggesting the presence of a glass transition during the gelatinization process (Lund & Lorenz, 1984) (Figure 3(b)). The optimized PPCS showed a minor shift in gelatinization peak temperature and a 1.11 J/g decrease in gelatinization enthalpy.

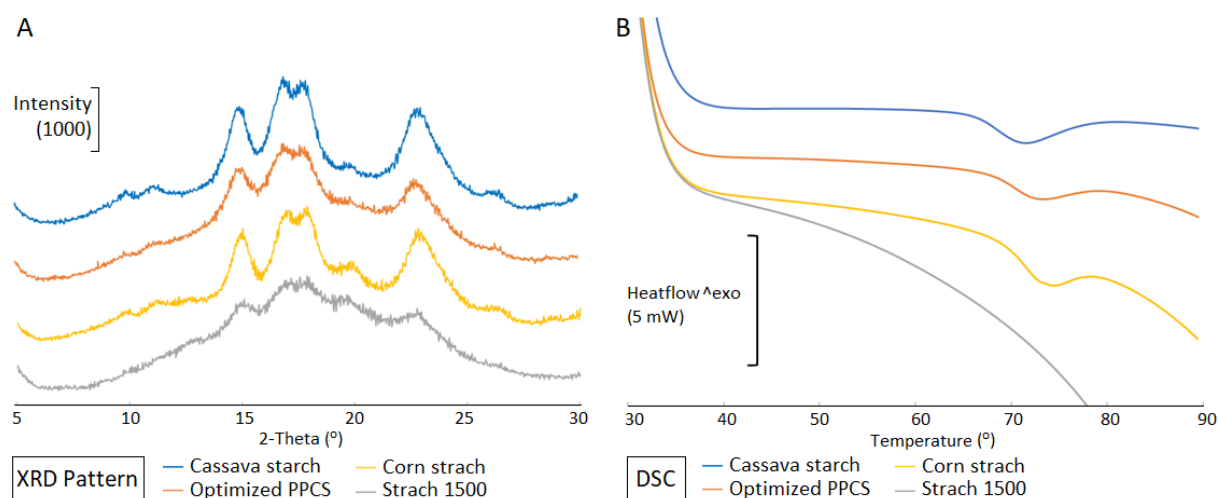


Figure 3. (A) XRD pattern and (B) DSC of cassava starch, optimized PPSC, corn starch, and Starch 1500®

This decrease in enthalpy is related to amylopectin crystallite disorder (Santos et al., 2018) and is supported by XRD observations. Using the Dome et. al. (2020) equation, the optimized PPSC has a gelatinization degree of 11.8%. Gelatinization temperature of cassava starch (shown in supplementary data) was also discovered to be different from that reported by Santos et. al. (2018) that is 65.6°C and by Dome et. al. (2020) that is 68.27°C. Starch 1500®, on the other hand, has no curves observed in the gelatinization area of corn starch.

CONCLUSION

All independent variables affect gelatinization related process, that is flow time, bulk density, tapped density, cold-water-soluble matter, and water absorption. The best combination for optimum process parameters was a starch moisture content of 39.9 percent, an extrusion temperature of 70°C, and a screw speed of 25.8 rpm. Compared to cassava starch, this combination of process parameter resulted in optimized PPSC with improved flowability, larger particle size, greater compactibility (though it still does not meet to the criteria), and higher water absorption capacities. Compared to Starch 1500®, the optimized PPSC has better flowability and similar water absorption capacity. The optimized PPSC contains a smaller percentage of cold-water soluble matter than Starch 1500®, implying that cassava starch does not undergo excessive gelatinization and can retain its crystallinity. This is supported by SEM, XRD, and DSC measurements. In

the future, optimized PPSC has the possibility to be used as a filler-binder in tablet formulation.

ACKNOWLEDGMENTS

The authors would like to gratefully thank the Saintek Scholarship. National Research and Innovation Agency of Indonesia that funded and supported this research.

REFERENCES

- Agarwal, S., & Chauhan, E. S. (2019). Extrusion processing: The effect on nutrients and based products. *The Pharma Innovation Journal*, 8(4), 464–470.
- Ali, S., Singh, B., & Sharma, S. (2020). Effect of processing temperature on morphology, crystallinity, functional properties, and in vitro digestibility of extruded corn and potato starches. *Journal of Food Processing and Preservation*, 44(7), e14531. <https://doi.org/10.1111/jfpp.14531>
- Anderson, R. A., Conway, H. F., & Peplinski, A. J. (1970). Gelatinization of corn grits by roll cooking, extrusion cooking and steaming. *Starch - Stärke*, 22(4), 130–135. <https://doi.org/10.1002/star.1970022048>
- Atkin, N. J., Abeysekera, R. M., & Robards, A. W. (1998). The events leading to the formation of ghost remnants from the starch granule surface and the contribution of the granule surface to the gelatinization endotherm. *Carbohydrate Polymers*, 36(2), 193–204. [https://doi.org/10.1016/S0144-8617\(98\)00002-2](https://doi.org/10.1016/S0144-8617(98)00002-2)

- Beakawi Al-Hashemi, H. M., & Baghabra Al-Amoudi, O. S. (2018). A review on the angle of repose of granular materials. *Powder Technology*, 330, 397–417. <https://doi.org/10.1016/j.powtec.2018.02.003>
- Bezerra, M. A., Santelli, R. E., Oliveira, E. P., Villar, L. S., & Escalera, L. A. (2008). Response surface methodology (RSM) as a tool for optimization in analytical chemistry. *Talanta*, 76(5), 965–977. <https://doi.org/10.1016/j.talanta.2008.05.019>
- Cheng, H., Wang, H., Ma, S., Xue, M., Li, J., & Yang, J. (2022). Development of a water solubility model of extruded feeds by utilizing a starch gelatinization model. *International Journal of Food Properties*, 25(1), 463–476. <https://doi.org/10.1080/10942912.2022.2046055>
- Council of Europe. (2010). *European pharmacopoeia*. (7th ed.). Council Of Europe: European Directorate for the Quality of Medicines and Healthcare.
- Divya, S., & Ganesh, G. N. K. (2019). Characterization of powder flowability using FT4–Powder Rheometer. *Journal of Pharmaceutical Sciences and Research*, 11(1), 25–29.
- Dome, K., Podgorbunskikh, E., Bychkov, A., & Lomovsky, O. (2020). Changes in the crystallinity degree of starch having different types of crystal structure after mechanical pretreatment. *Polymers*, 12(3), Article 3. <https://doi.org/10.3390/polym12030641>
- European Pharmacopoeia. (2010). Powder Flow <2.9.36>. In *European Pharmacopoeia* (6th ed.). Directorate for the Quality of Medicines of the Council of Europe.
- Getachew, A., Yilma, Z., & Abrha, S. (2020). Acetylation and evaluation of taro boloso-I starch as directly compressible excipient in tablet formulation. *Advances in Pharmacological and Pharmaceutical Sciences*, 2020, 2708063. <https://doi.org/10.1155/2020/2708063>
- Iqbal, M. K., Singh, P. K., Shuaib, M., Iqbal, A., & Singh, M. (2014). Recent advances in direct compression technique for pharmaceutical tablet formulation. *International Journal of Pharmaceutical Research and Development*, 6(1), 049–057.
- Jiang, H., Jane, J.-L., Acevedo, D., Green, A., Shinn, G., Schrenker, D., Srichuwong, S., Campbell, M., & Wu, Y. (2010). Variations in starch physicochemical properties from a generation-means analysis study using amylo maize V and VII parents. *Journal of Agricultural and Food Chemistry*, 58(9), 5633–5639. <https://doi.org/10.1021/jf904531d>
- Jivraj, M., Martini, L. G., & Thomson, C. M. (2000). An overview of the different excipients useful for the direct compression of tablets. *Pharmaceutical Science & Technology Today*, 3(2), 58–63. [https://doi.org/10.1016/s1461-5347\(99\)00237-0](https://doi.org/10.1016/s1461-5347(99)00237-0)
- Kaleem, M. A., Alam, M. Z., Khan, M., Jaffery, S. H. I., & Rashid, B. (2021). An experimental investigation on accuracy of Hausner Ratio and Carr Index of powders in additive manufacturing processes. *Metal Powder Report*, 76, S50–S54. <https://doi.org/10.1016/j.mprp.2020.06.061>
- Karisma Sari, K. L., Anton Prasetya, I. G. N. J., & Sri Arisanti, Cok. I. (2012). Pengaruh rasio amilum:air dan suhu pemanasan terhadap sifat fisik amilum singkong pregelatin yang ditujukan sebagai eksipien tablet. *Jurnal Farmasi Udayana*, 1(1), 50–67.
- Leonel, M., Freitas, T. S. de, & Mischán, M. M. (2009). Physical characteristics of extruded cassava starch. *Scientia Agricola*, 66, 486–493. <https://doi.org/10.1590/S0103-90162009000400009>
- Lund, D., & Lorenz, K. J. (1984). Influence of time, temperature, moisture, ingredients, and processing conditions on starch gelatinization. *C R C Critical Reviews in Food Science and Nutrition*, 20(4), 249–273. <https://doi.org/10.1080/10408398409527391>
- Mishra, A., Kumar, S., & Kumar, S. (2008). Application of Box-Benkhken experimental design for optimization of laccase production by *Coriolus versicolor* MTCC138 in solid-state fermentation. *Journal of Scientific and Industrial Research*, 67.
- Odeku, O. A., & Picker-Freyer, K. M. (2009). Characterization of acid modified Dioscorea starches as direct compression excipient. *Pharmaceutical Development and Technology*, 14(3), 259–270.

- <https://doi.org/10.1080/10837450802572367>
- Okunlola, A. (2018). Flow, compaction and tableting properties of co-processed excipients of pregelatinized Ofada rice starch and HPMC. *Journal of Excipients and Food Chemicals*, 9(1). <https://jefc.scholasticahq.com/article/3405-flow-compaction-and-tableting-properties-of-co-processed-excipients-of-pregelatinized-ofada-rice-starch-and-hpmc>
- Park, S., & Kim, Y.-R. (2021). Clean label starch: Production, physicochemical characteristics, and industrial applications. *Food Science and Biotechnology*, 30(1), 1–17. <https://doi.org/10.1007/s10068-020-00834-3>
- Putra, M. W. (2011). *Amprotab® pregelatin sebagai bahan pengisi pengikat dalam pembuatan tablet dengan metode kempa langsung* [Thesis]. Universitas Islam Indonesia.
- Rashid, I., Omari, M. M. H. A., & Badwan, A. A. (2013). From native to multifunctional starch-based excipients designed for direct compression formulation. *Starch - Stärke*, 65(7–8), 552–571. <https://doi.org/10.1002/star.201200297>
- Rojas, J., Uribe, Y., & Zuluaga, A. (2012). Powder and compaction characteristics of pregelatinized starches. *Die Pharmazie*, 67(6), 513–517.
- Šantl, M., Ilić, I., Vrečer, F., & Baumgartner, S. (2011). A compressibility and compactibility study of real tableting mixtures: The impact of wet and dry granulation versus a direct tableting mixture. *International Journal of Pharmaceutics*, 414(1–2), 131–139. <https://doi.org/10.1016/j.ijpharm.2011.05.025>
- Santos, T. P. R. d., Franco, C. M. L., Demiate, I. M., Li, X., Garcia, E. L., Jane, J.-L., & Leonel, M. (2018). Spray-drying and extrusion processes: Effects on morphology and physicochemical characteristics of starches isolated from Peruvian carrot and cassava. *International Journal of Biological Macromolecules*, 118, 1346–1353. <https://doi.org/10.1016/j.ijbiomac.2018.06.070>
- Short, R. W. P., & Verbanac, F. (1978). *Precompacted-starch binder-disintegrant-filler material for direct compression tablets and dry dosage capsules* (United States Patent No. US4072535A). <https://patents.google.com/patent/US4072535/en?q=u.s.+4%2c072%2c535>
- Sørensen, M. (2012). A review of the effects of ingredient composition and processing conditions on the physical qualities of extruded high-energy fish feed as measured by prevailing methods. *Aquaculture Nutrition*, 18(3), 233–248. <https://doi.org/10.1111/j.1365-2095.2011.00924.x>
- Sulaiman, T. N. S., Wahyuono, W., Bestari, A. N., & Aziza, F. N. (2022). Preparation and characterization of Pregelatinized Sago Starch (PSS) from Native Sago Starch (NSS) (Metroxylon sp.) and its evaluation as tablet disintegrant and filler-binder on direct compression tablet. *Indonesian Journal of Pharmacy*, 33(2), 251–260. <https://doi.org/10.22146/ijp.3543>
- Suñé Negre, J. M., Roig Carreras, M., García, R. F., Montoya, E. G., Lozano, P. P., Aguilar, J. E., Carmona, M. M., & Ticó Grau, J. R. (2013). 5 - SeDeM Diagram: An expert system for preformation, characterization and optimization of tablets obtained by direct compression. In J. E. Aguilar (Ed.), *Formulation Tools for Pharmaceutical Development* (pp. 109–135). Woodhead Publishing. <https://doi.org/10.1533/9781908818508.109>
- Swinkels, J. J. M. (1985). Composition and properties of commercial native starches. *Starch - Stärke*, 37(1), 1–5. <https://doi.org/10.1002/star.19850370102>
- U.S. Pharmacopeia. (2018). *The United States Pharmacopeia, USP 41/The National Formulary, NF 36*. MD United States Pharmacopeial Convention.
- Wootton, M., & Bamunuarachchi, A. (1978). Water binding capacity of commercial produced native and modified starches. *Starch - Stärke*, 30(9), 306–309. <https://doi.org/10.1002/star.19780300905>
- Xia, W., Wang, F., Li, J., Wei, X., Fu, T., Cui, L., Li, T., & Liu, Y. (2015). Effect of high speed jet on the physical properties of tapioca starch. *Food Hydrocolloids*, 49, 35–41. <https://doi.org/10.1016/j.foodhyd.2015.03.010>

Zhang, X., Tong, Q., Zhu, W., & Ren, F. (2013). Pasting, rheological properties and gelatinization kinetics of tapioca starch with sucrose or glucose. *Journal of Food Engineering*, 114(2), 255–261. <https://doi.org/10.1016/j.jfoodeng.2012.08.002>

Zhang, Y., Xiao, C., Bindzus, W., & Green, V. (2006). *Tablet excipient* (United States Patent No. US20060008521A1). <https://patents.google.com/patent/US20060008521A1/en>